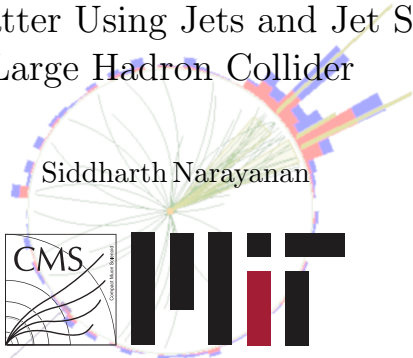


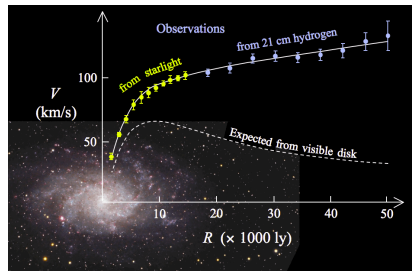
# Searching for Dark Matter Using Jets and Jet Substructure at the Large Hadron Collider



Ph.D. Thesis Defense - 2019/01/24

# Dark matter - in space

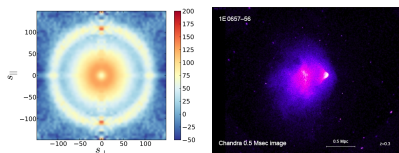
Strong astrophysical evidence for DM:



[1,2]



[3]

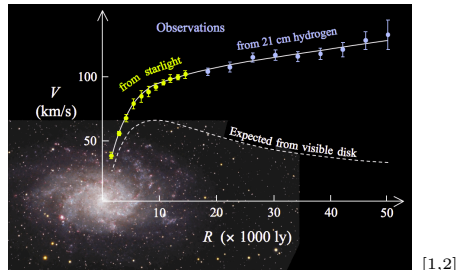


[4]

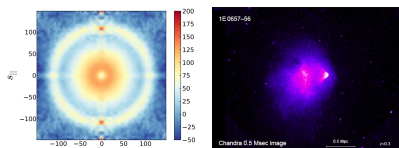
[5]

# Dark matter - in space

Strong astrophysical evidence for DM:



[3]



Weakly Interacting Massive Particles

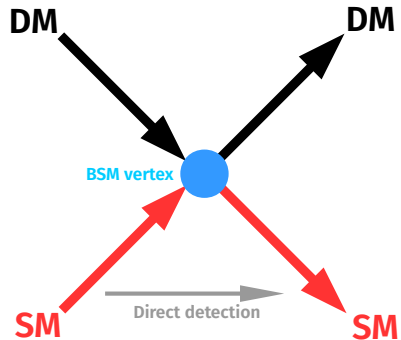
- ▶ Weakly: DM-SM coupling  $g_\chi \sim g$
- ▶ Massive: mass  $m_\chi \sim 100$  GeV
- ▶ The “WIMP miracle”:

$$\Omega \propto \frac{\rho}{\rho_c} \propto \frac{1}{\langle \sigma v \rangle}$$

$$\Omega_{\text{meas.}} = 0.12, \quad \Omega_\chi \sim 0.1$$

- ▶ Almost any DM model probed by a collider has a WIMP
- ▶ Many other models exist (axions, MACHOs, ...)

# Dark matter - in a laboratory



Search for DM-SM interactions as Earth moves through DM halo

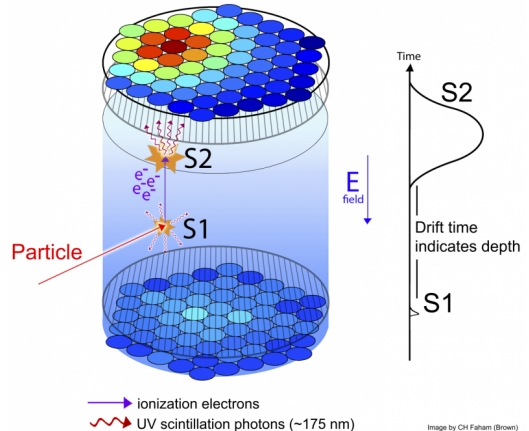
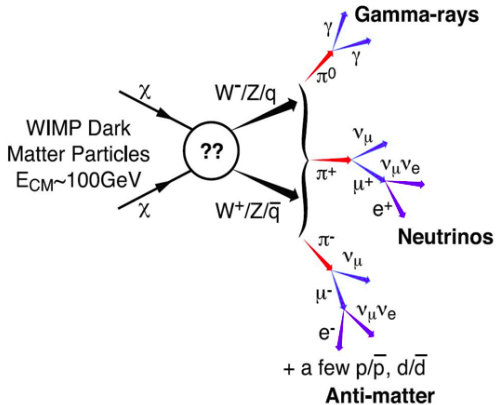
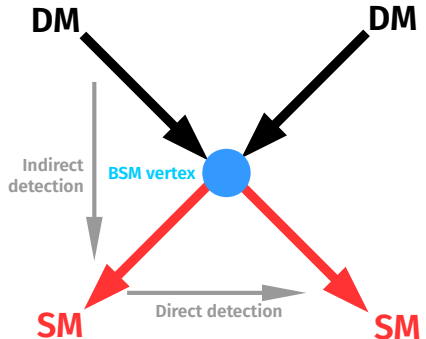


Image by CH Faham (Brown)

[6]

LUX (shown), PandaX, CDMS, Xenon1T,...

# Dark matter - in a laboratory

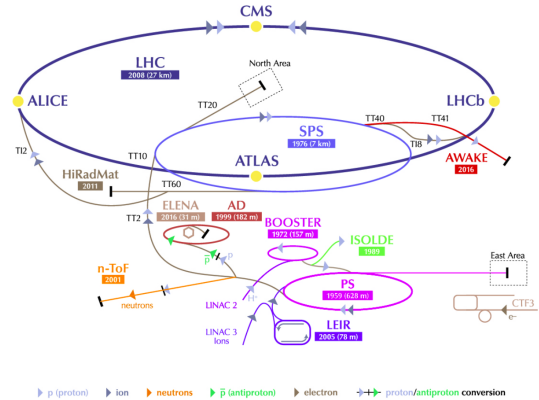
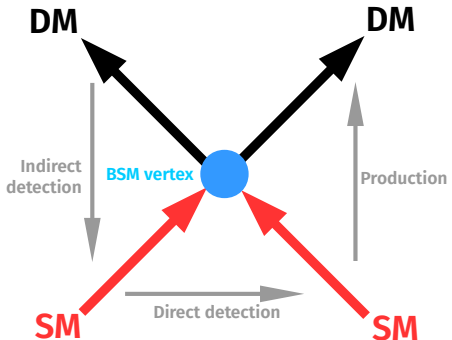


[7]

FermiLAT, AMS

Look for SM remnants of DM-DM  
annihilation in space

# Dark matter - in a laboratory

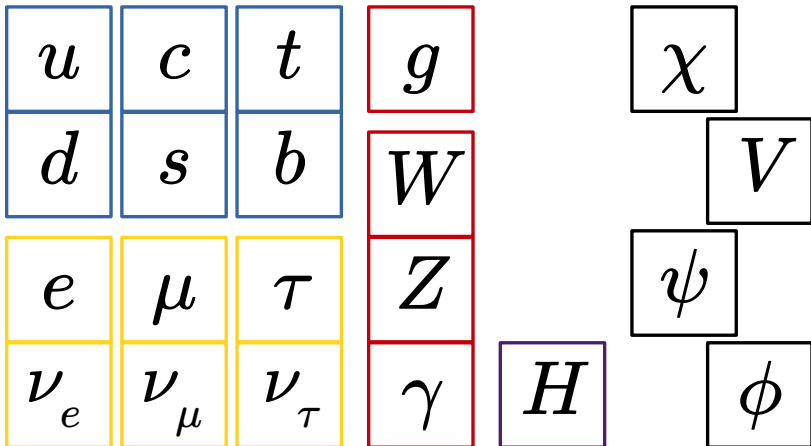


Exploit DM-SM interaction to produce DM  
in a laboratory

# Production of WIMPs at a hadron collider

Effective coupling to quarks/gluons  $\gtrsim 10^{-4}$

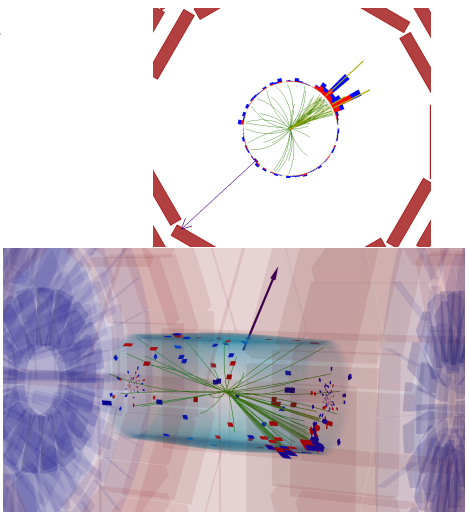
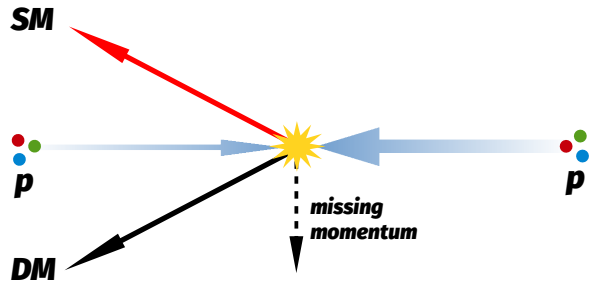
Masses  $\lesssim \sqrt{s}$



# Seeing the invisible at a hadron collider



- ▶ By definition, DM will not interact with a detector
- ▶ Look for production of DM with SM particle(s)
- ▶ Key observable is transverse momentum imbalance



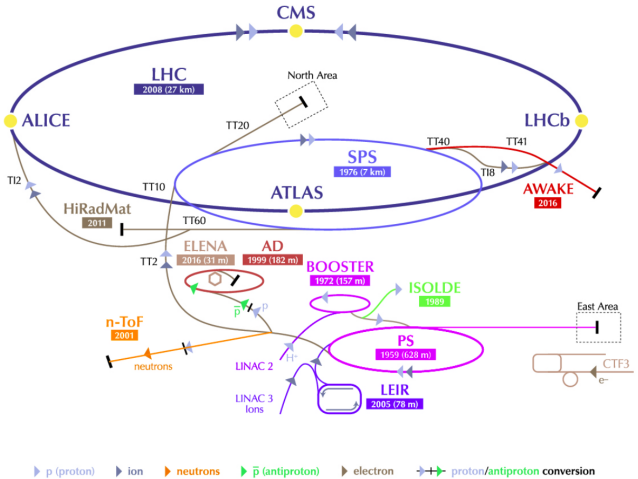
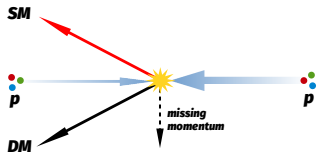
# Which SM particle(s)?

Many to choose from. SM particle choice  $\Leftrightarrow$  type of DM you can look for

	SM particle	Minimal extension	Higgs-like	Extra dimensions	Extended Higgs sector	Flavor violation
Quarks	$q(g)$					
	$t$					
	$qq'$					
	$t\bar{t}$					
	$b/b\bar{b}$					
Gauge bosons	$\gamma$					
	$V \rightarrow q\bar{q}'$					
	$Z \rightarrow \ell^+\ell^-$					
Higgs	$H \rightarrow x\bar{x}$					

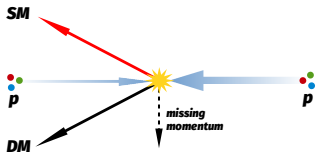
# $p_T^{\text{miss}}$ at the LHC

- CMS records collisions from the LHC
  - Today:  $\sqrt{s} = 13 \text{ TeV}$   $pp$  collision data from 2016
- Missing momentum:



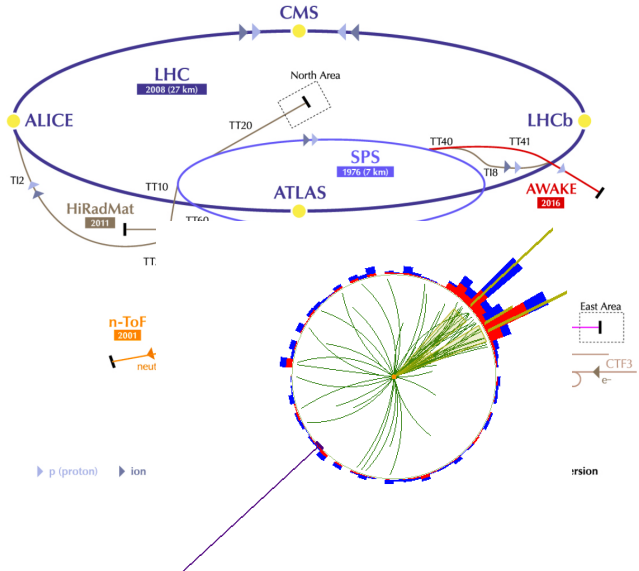
# $p_T^{\text{miss}}$ at the LHC

- CMS records collisions from the LHC
  - Today:  $\sqrt{s} = 13 \text{ TeV}$   $pp$  collision data from 2016
- Missing momentum:



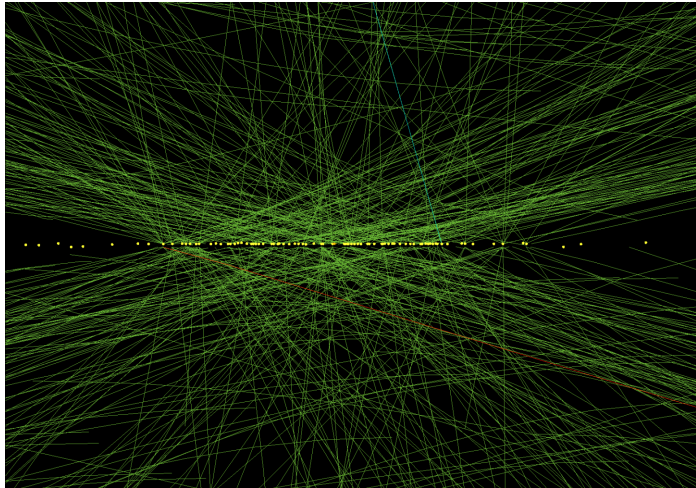
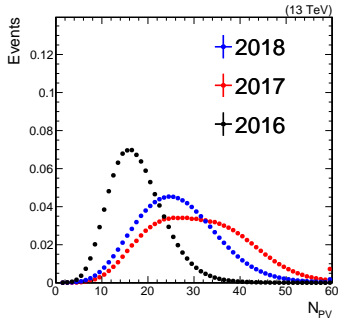
- turns into:

$$\vec{p}_T^{\text{miss}} = - \sum_{i \in \text{particles}} \vec{p}_{T,i}$$



# Proton collisions

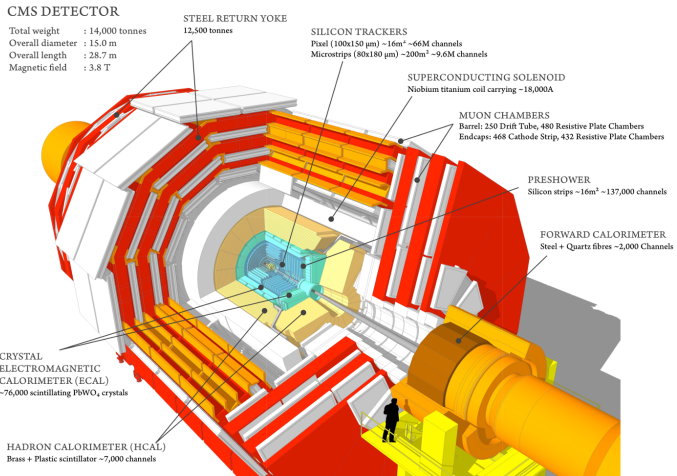
- ▶ Two 6.5 TeV proton beams
- ▶  $\sim 10^{11}$  protons per bunch
- ▶ Average collision has 10-25 pile-up interactions



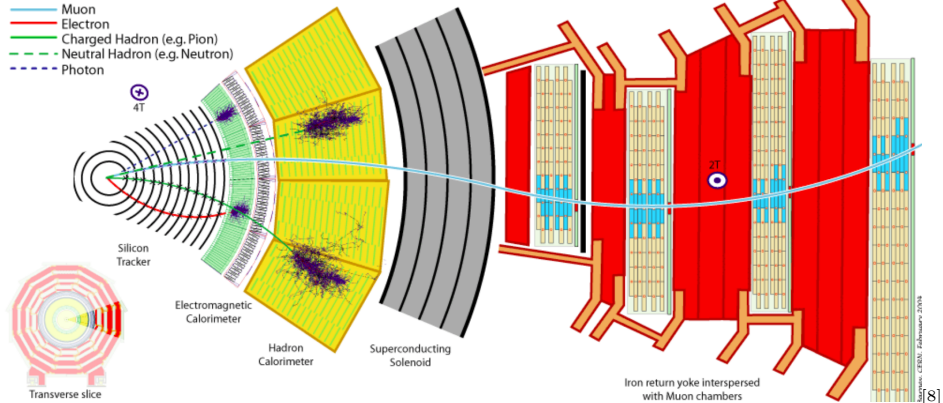
# Compact Muon Solenoid

All particles in sum  $\Rightarrow$   
all subdetectors help measure  $p_T^{\text{miss}}$ !

- ▶ Solenoidal magnet
  - ▶ 3.8 T B field
- ▶ Silicon tracker
  - ▶ Charged particles'  $\vec{p}$
  - ▶ Track vertices
- ▶ Calorimeters
  - ▶ EM and hadronic
  - ▶ Good energy resolution
  - ▶ Large coverage
- ▶ Muon chambers
  - ▶ ID muons
  - ▶ Help measure  $\vec{p}$



# Particle reconstruction



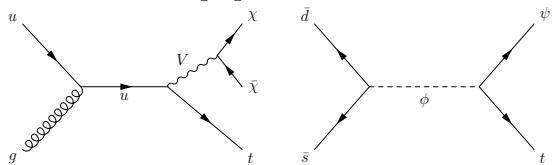
Tracker	ECAL	HCAL	Muon
$ \eta  < 2.5$ $\frac{0.015\% \cdot p_T}{\text{GeV}} \oplus 0.5\%$	$ \eta  < 3$ $\frac{3\%}{\sqrt{E/\text{GeV}}} \oplus \frac{12\%}{E/\text{GeV}} \oplus 0.3\%$	$ \eta  < 5$ $\frac{85\%}{\sqrt{E/\text{GeV}}} \oplus 7.4\%$	$ \eta  < 2.4$ 3% at 100 GeV

# Outline of this talk

## DM production mode

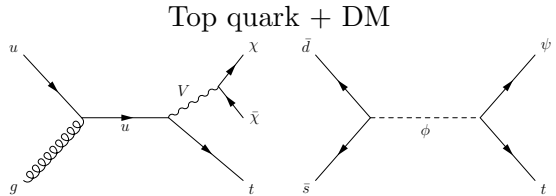
## Highlights

Top quark + DM



# Outline of this talk

## DM production mode



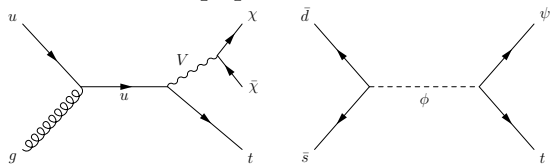
## Highlights

Jet substructure  
Invisible background estimation

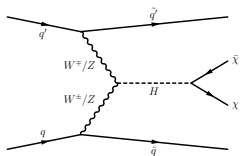
# Outline of this talk

## DM production mode

### Top quark + DM



### Higgs $\rightarrow$ DM



## Highlights

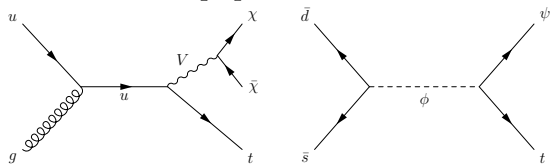
Jet substructure

Invisible background estimation

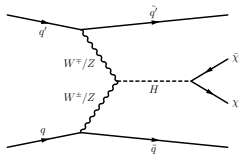
# Outline of this talk

## DM production mode

### Top quark + DM



### Higgs $\rightarrow$ DM



## Highlights

Jet substructure  
Invisible background estimation

Forward jets

Electroweak SM backgrounds

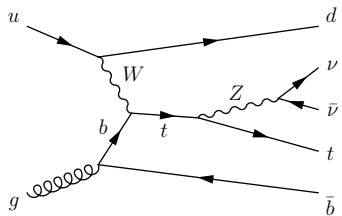
# Mono-Top

# Hallmarks of top quark+ $p_T^{\text{miss}}$

- ▶ Final state violates flavor conservation
  - ▶ SM will have  $b$  quark in the final state
- ▶ Excess mono-top production  $\Rightarrow$  flavor-changing BSM

# Hallmarks of top quark+ $p_T^{\text{miss}}$

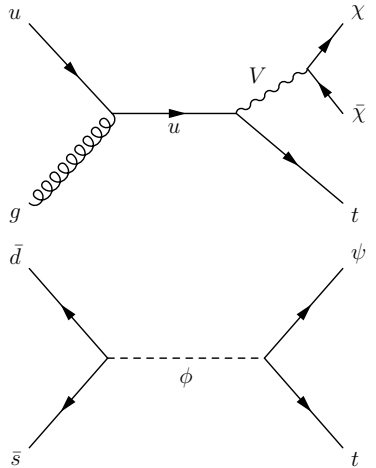
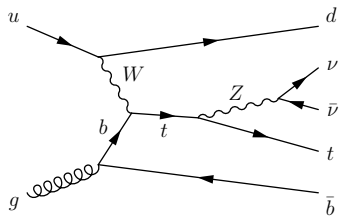
- ▶ Final state violates flavor conservation
  - ▶ SM will have  $b$  quark in the final state
- ▶ Excess mono-top production  $\Rightarrow$  flavor-changing BSM
- ▶ Leading SM process: 0.14 pb  $\Rightarrow$  5000 events in 36/fb



## Hallmarks of top quark+ $p_T^{\text{miss}}$

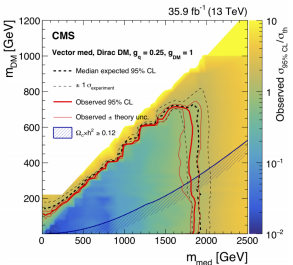
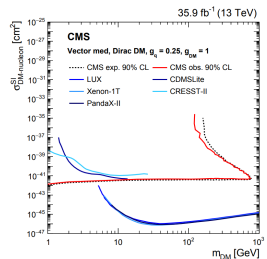
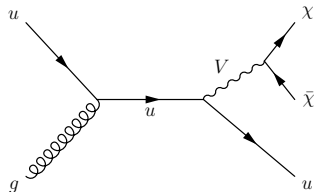


- ▶ Final state violates flavor conservation
    - ▶ SM will have  $b$  quark in the final state
  - ▶ Excess mono-top production  $\Rightarrow$  flavor-changing BSM
  - ▶ Leading SM process:  $0.14 \text{ pb} \Rightarrow 5000 \text{ events in } 36/\text{fb}$

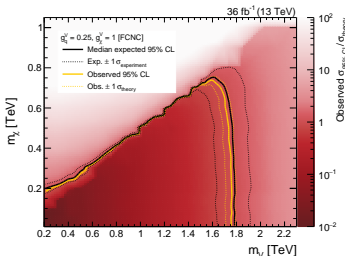
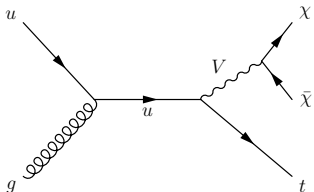


# Connection to other DM models

Flavor conserving: diagonal  $g_u^V$

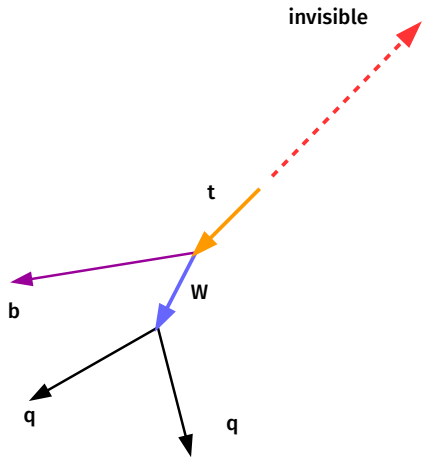


Flavor violating: off-diagonal  $g_u^V$



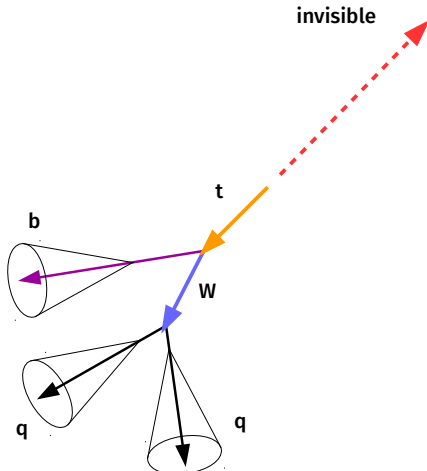
# Anatomy of a mono-top event

Hadronic decay  $\Rightarrow$  larger  $\mathcal{B}$ , no  $p_T^{\text{miss}}$



# Anatomy of a mono-top event

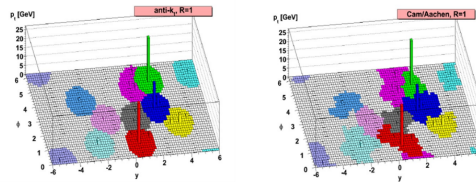
Quarks shower and hadronize into jets



- Particles are clustered into jets based on a distance metric:

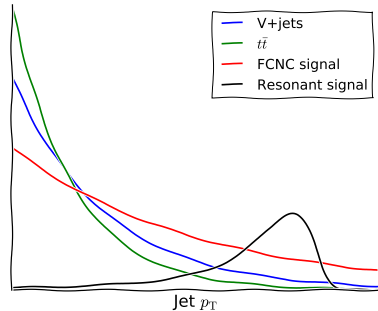
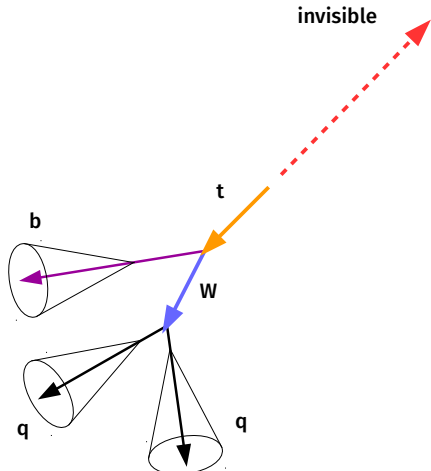
$$d_{ij} = \min\{p_{T,i}^{2q}, p_{T,j}^{2q}\} \frac{\Delta R(p_i^\mu, p_j^\mu)^2}{R}$$

- $q = -1$ : anti- $k_T$  (AK)
- $q = 0$ : Cambridge-Aachen (CA)
- Single-parton jet: AK  $R = 0.4$



# Anatomy of a mono-top event

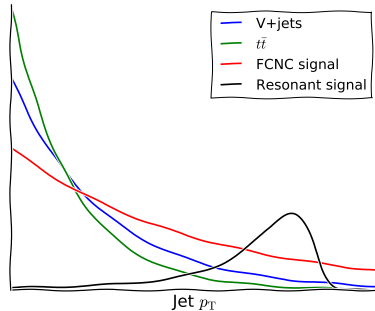
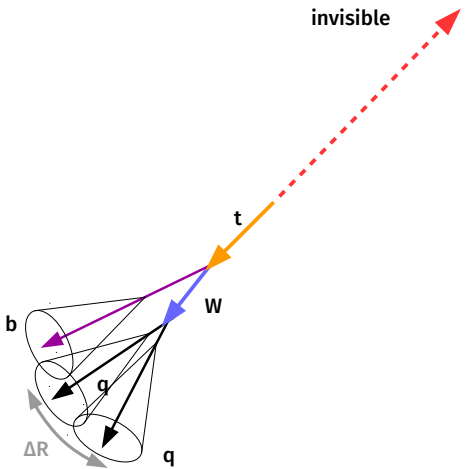
Quarks shower and hadronize into jets



- ▶ Signal more energetic than SM
- ▶ Maximize S/B  $\Rightarrow$  large jet  $p_T$

# Anatomy of a mono-top event

Decay products collimate

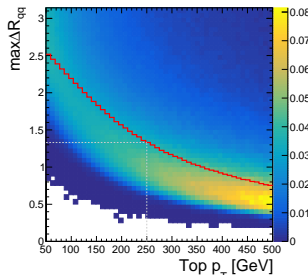


- ▶ Signal more energetic than SM
- ▶ Maximize S/B  $\Rightarrow$  large jet  $p_T$
- ▶ Separation between jets:  $\Delta R \sim 2m_t/p_T$ 
  - ▶  $p_T > 250 \text{ GeV} \Rightarrow$  jets ( $R = 0.4$ ) overlap
  - ▶  $\Delta R = \sqrt{(\Delta\phi)^2 + (\Delta\eta)^2}$

# Reconstruction of top quark jet

## Clustering

- ▶ Three AK  $R = 0.4$  jets  $\rightarrow$   
single CA  $R = 1.5$  jet

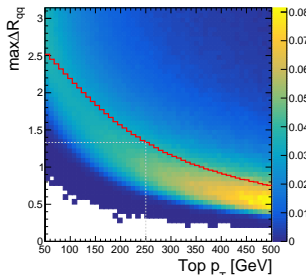


- ▶ These are huge jets: half  
the detector!
- ▶ Many extra particles

# Reconstruction of top quark jet

## Clustering

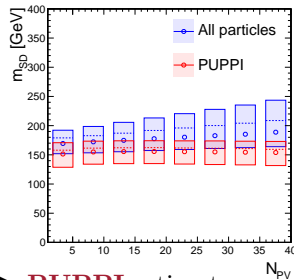
- ▶ Three AK  $R = 0.4$  jets  $\rightarrow$  single CA  $R = 1.5$  jet



- ▶ These are huge jets: half the detector!
- ▶ Many extra particles

## Pileup particles

- ▶ 10-25 vertices per collision
- ▶ PU particles are isotropic

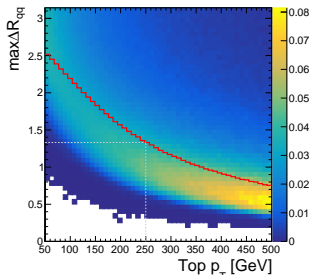


- ▶ **PUPPI** estimates  
 $P(\text{PU}|p_T, \eta, \phi)$  from proximity to PV particles

# Reconstruction of top quark jet

## Clustering

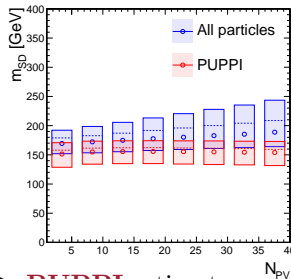
- ▶ Three AK  $R = 0.4$  jets  $\rightarrow$  single CA  $R = 1.5$  jet



- ▶ These are huge jets: half the detector!
- ▶ Many extra particles

## Pileup particles

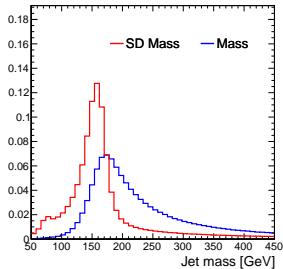
- ▶ 10-25 vertices per collision
- ▶ PU particles are isotropic



- ▶ **PUPPI** estimates  $P(\text{PU}|p_T, \eta, \phi)$  from proximity to PV particles

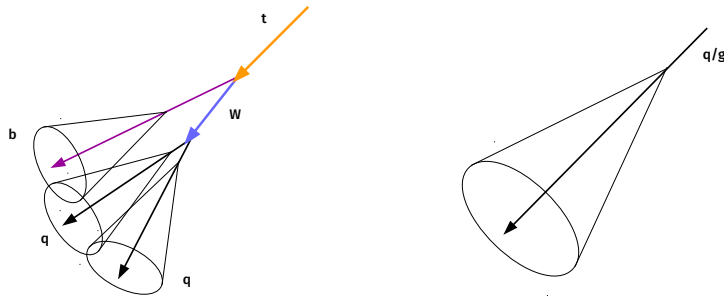
## Non-PS radiation

- ▶ ISR, UE, MPI



- ▶ **Soft drop** removes wide-angle and soft radiation from jet

- Top quark  $\rightarrow 3q \Rightarrow$  top jet has 3 “prongs”: regions of correlated radiation



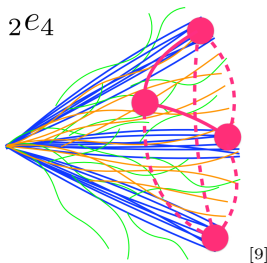
- **Substructure** observables are sensitive to such features
  - $N$ -subjettiness, subjet algorithms, ECFs,...

# Energy correlation functions

ECFs are **N**-point distance-weighted correlation functions among particles of the jet

$$e(a, \mathbf{N}, \alpha) \sim \sum_{\mathbf{N} \text{ particles } \in J}$$

sets of **N** particles

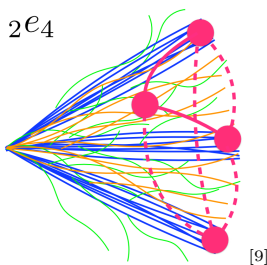


# Energy correlation functions

ECFs are **N**-point distance-weighted correlation functions among particles of the jet

$$e(a, \mathbf{N}, \alpha) \sim \sum_{\mathbf{N} \text{ particles } \in J} \left[ \prod_{p \in \text{particles}} \frac{E_p}{E_J} \right]$$

sets of **N** particles    energy fractions

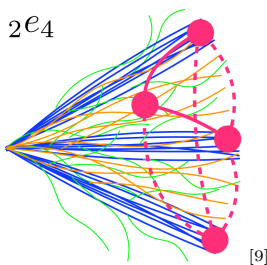


# Energy correlation functions

ECFs are **N**-point distance-weighted correlation functions among particles of the jet

$$e(a, \mathbf{N}, \alpha) \sim \sum_{\mathbf{N} \text{ particles } \in J} \left[ \prod_{p \in \text{particles}} \frac{E_p}{E_J} \right] \times \min \left\{ \prod_{p,q \in \text{particles}}^a \theta(p, q) \right\}^\alpha$$

sets of **N** particles      energy fractions      opening angle

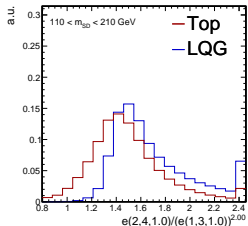
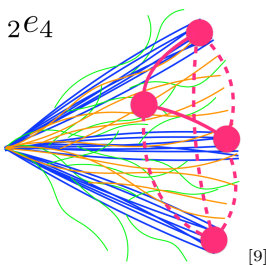


# Energy correlation functions

ECFs are **N**-point distance-weighted correlation functions among particles of the jet

$$e(a, \mathbf{N}, \alpha) \sim \sum_{\mathbf{N} \text{ particles } \in J} \left[ \prod_{p \in \text{particles}} \frac{E_p}{E_J} \right] \times \min \left\{ \prod_{p,q \in \text{particles}}^a \theta(p, q) \right\}^\alpha$$

sets of **N** particles
energy fractions
opening angle



$$e(4)/e(3)$$

# Energy correlation functions

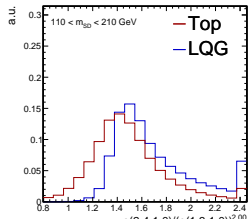
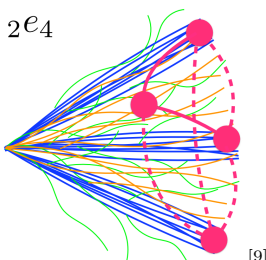
ECFs are **N**-point distance-weighted correlation functions among particles of the jet

$$e(a, \mathbf{N}, \alpha) \sim \sum_{\mathbf{N} \text{ particles } \in J} \left[ \prod_{p \in \text{particles}} \frac{E_p}{E_J} \right] \times \min \left\{ \prod_{p,q \in \text{particles}}^a \theta(p, q) \right\}^\alpha$$

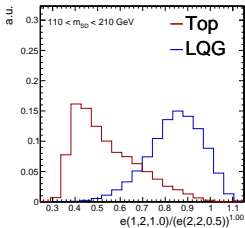
sets of **N** particles

energy fractions

opening angle



$e(4)/e(3)$



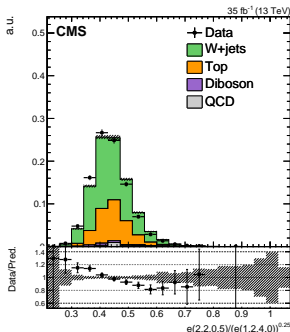
$e(2)/e(2)$

# Building a combined tagger

## Modeling issues

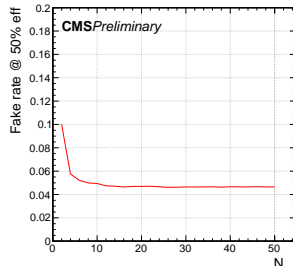
$$\frac{e(a, N, \alpha)}{e(b, M, \beta)^x}, \quad M \leq N, \quad x = \frac{a\alpha}{b\beta}$$

- ▶ Some ECF ratios poorly described by PS model



## Dimensional reduction

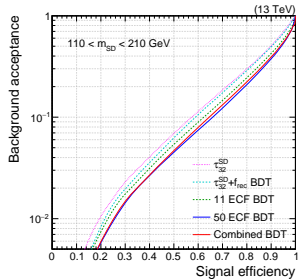
- ▶ Large ECF ratio space
- ▶ Expensive to compute



- ▶ Embed dimensional reduction into boosted decision tree training

## Combined tagger

- ▶ Final discriminator combines ECFs,  $\tau_{32}$ ,  $f_{rec}$



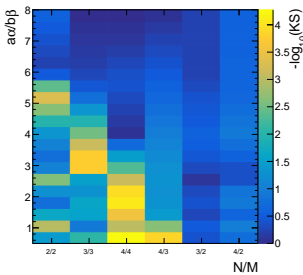
- ▶ 30% better background rejection than  $\tau_{32}$

# Building a combined tagger

## Modeling issues

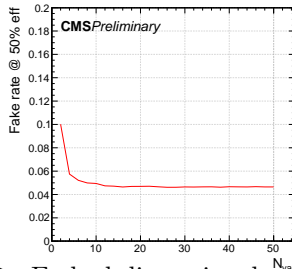
$$\frac{e(a, N, \alpha)}{e(b, M, \beta)^x}, \quad M \leq N, \quad x = \frac{a\alpha}{b\beta}$$

- ▶ Some ECF ratios poorly described by PS model



## Dimensional reduction

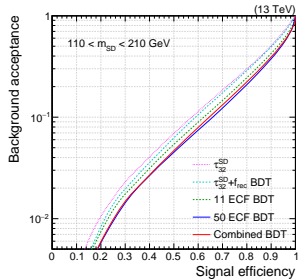
- ▶ Large ECF ratio space
- ▶ Expensive to compute



- ▶ Embed dimensional reduction into boosted decision tree training

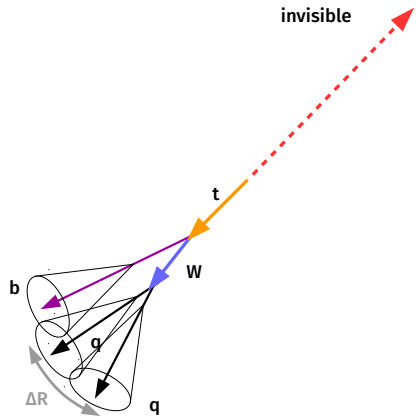
## Combined tagger

- ▶ Final discriminator combines ECFs,  $\tau_{32}$ ,  $f_{\text{rec}}$



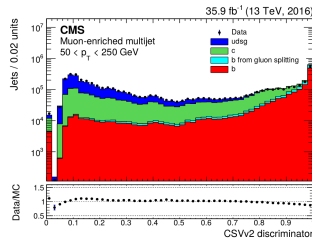
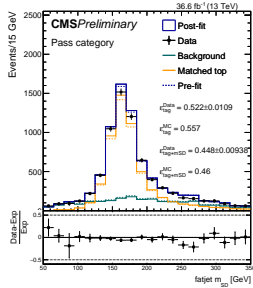
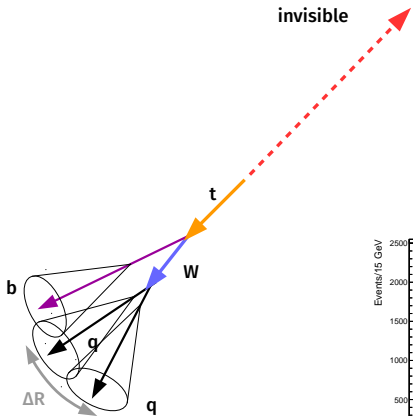
- ▶ 30% better background rejection than  $\tau_{32}$

# Selecting mono-top events



- ▶  $p_T^{\text{miss}} > 250 \text{ GeV}$  (trigger)
- ▶ No  $e, \mu, \tau_h$ , and AK4  $b$  jets
- ▶ One CA15 jet,  $p_T > 250 \text{ GeV}$
- ▶ Selected by BDT

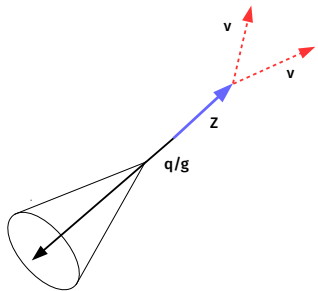
# Selecting mono-top events



- ▶  $p_T^{\text{miss}} > 250 \text{ GeV}$  (trigger)
- ▶ No  $e, \mu, \tau_h$ , and AK4  $b$  jets
- ▶ One CA15 jet,  $p_T > 250 \text{ GeV}$ 
  - ▶ Selected by BDT
  - ▶ Mass consistent with  $m_t$
  - ▶ Signature of  $B$  meson decay inside jet
- ▶ Lab frame  $c\tau \sim \mathcal{O}(\text{mm})$

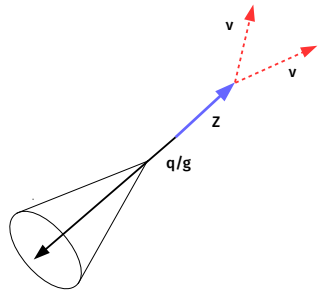
# SM backgrounds

$Z \rightarrow \nu\nu$  (30%)

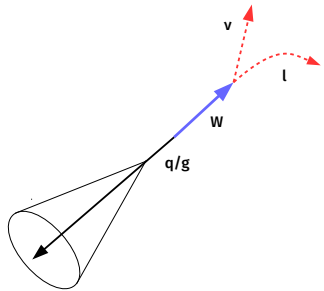


# SM backgrounds

$Z \rightarrow \nu\nu$  (30%)

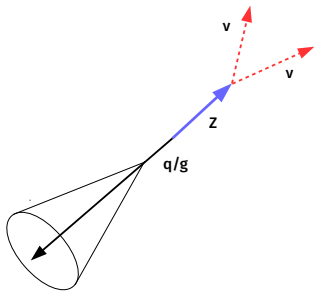


$W \rightarrow (\ell)\nu$  (15%)

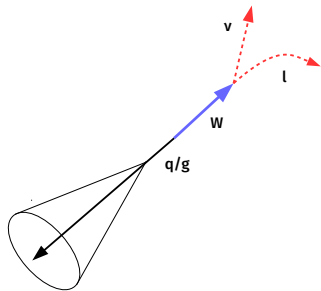


# SM backgrounds

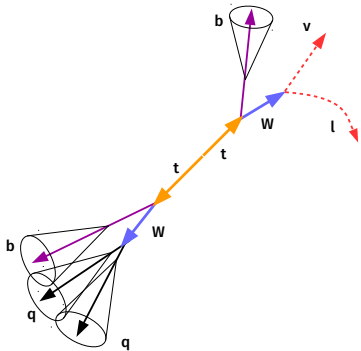
$Z \rightarrow \nu\nu$  (30%)



$W \rightarrow (\ell)\nu$  (15%)

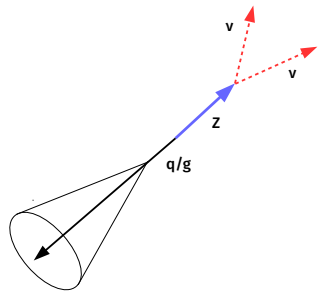


$t$  quark pair (50%)

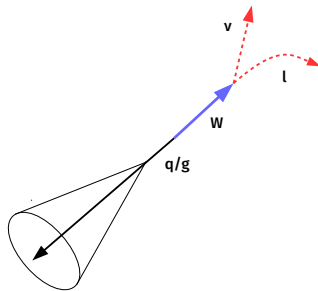


# SM backgrounds

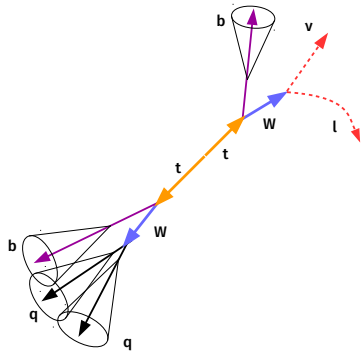
$Z \rightarrow \nu\nu$  (30%)



$W \rightarrow (\ell)\nu$  (15%)



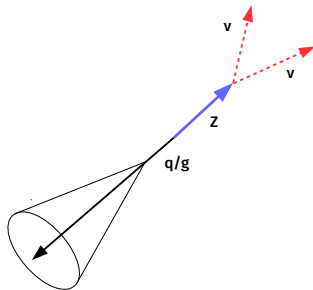
$t$  quark pair (50%)



Note that  $p_T^{\text{miss}}$  is the transverse momentum of the **vector boson**

# Prediction of $Z$ $p_T^{\text{miss}}$ spectrum

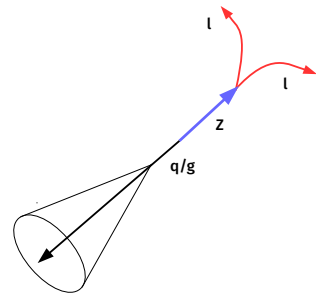
- MC predictions have  $\sim 30\%$  uncertainties  $\Rightarrow$  use data to constrain
- $p_T^{\text{miss}}$  is driven by jet measurement
- **Hadronic recoil ( $U$ )**  $\equiv$  momentum imbalance if we pretend  $\ell^\pm, \gamma$  are invisible.



$Z \rightarrow \nu\nu$  (20.5%)

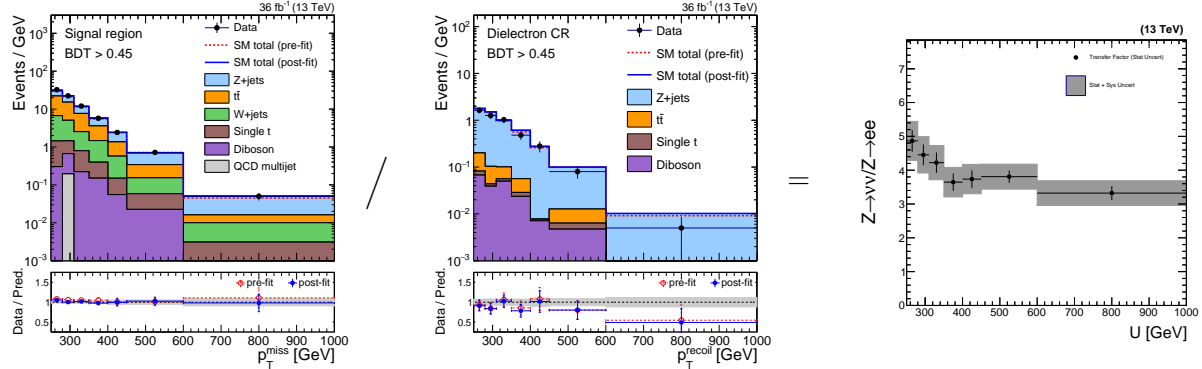
$$p_T^{\text{miss}} \longleftrightarrow p_T^{\text{miss}}(\text{no } \ell)$$

In both cases:  
 $U \approx p_T^Z$



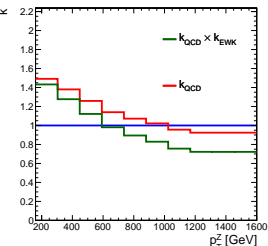
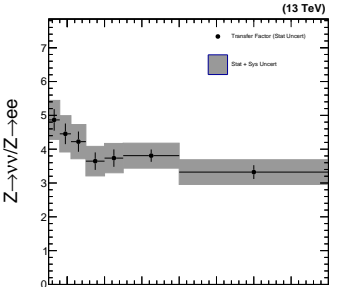
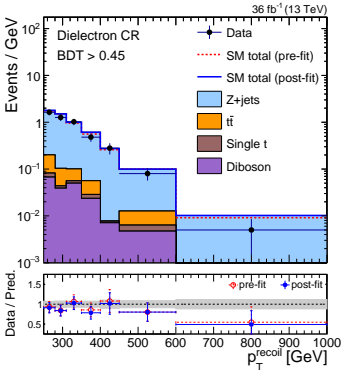
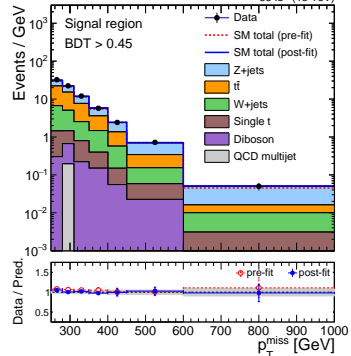
$Z \rightarrow \ell\ell$  (6.8%)

# The real observable: $T = Z(\rightarrow \nu\nu)/Z(\rightarrow \ell\ell)$



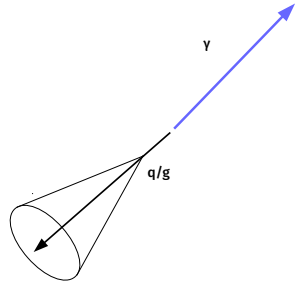
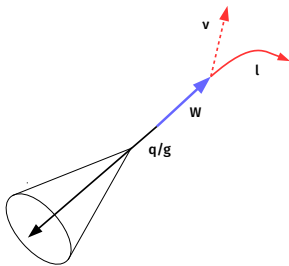
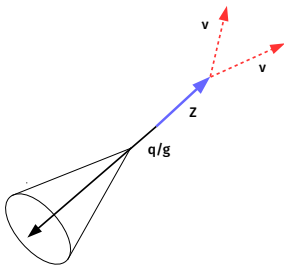
- ▶ Exp. and MC stat. uncertainties are small ( $\leq 7\%$ )
- ▶ Jet-related experimental uncertainties cancel
- ▶ Data stat. uncertainties are large at high  $U$

# The real observable: $T = Z(\rightarrow \nu\nu)/Z(\rightarrow \ell\ell)$



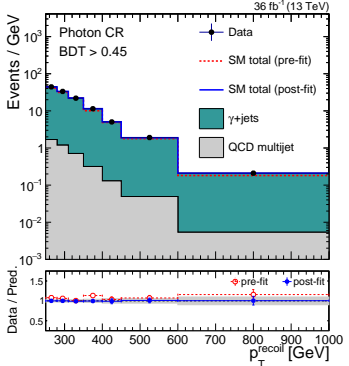
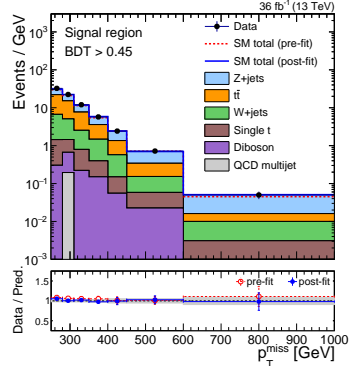
- ▶ Exp. and MC stat. uncertainties are small ( $\leq 7\%$ )
- ▶ Jet-related experimental uncertainties cancel
- ▶ Data stat. uncertainties are large at high  $U$
- ▶ Compare to LO-to-NLO effect (+40% to -30%)

# Additional constraints: $Z/\gamma$ , $Z/W$

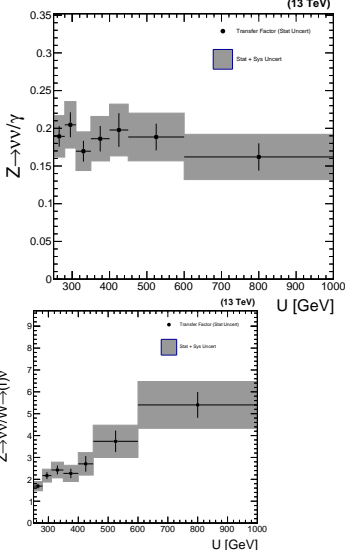


- ▶ Higher-order corrections needed for  $Z/\gamma$  and  $Z/W$  predictions
- ▶ Total (partial) cancellation of jet (theory) uncertainties

# Additional constraints: $Z/\gamma$ , $Z/W$

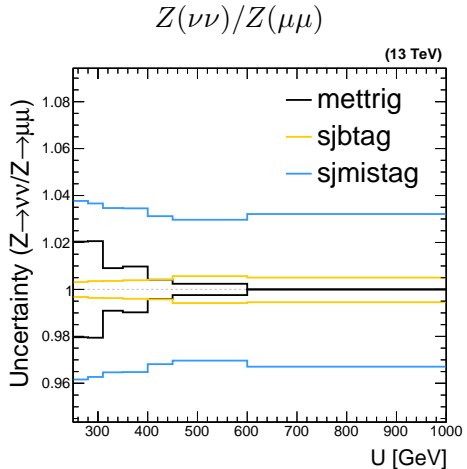


=

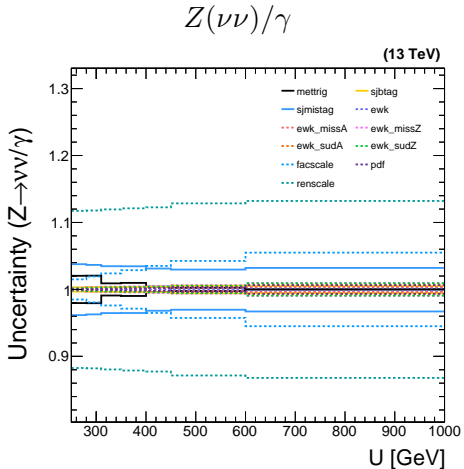


- ▶ Higher-order corrections needed for  $Z/\gamma$  and  $Z/W$  predictions
- ▶ Total (partial) cancellation of jet (theory) uncertainties
- ▶ Small data stat. uncertainties

# Extrapolation uncertainties



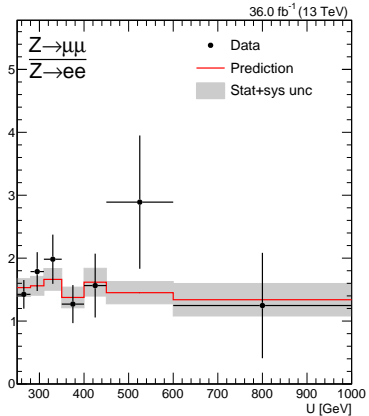
Small experimental uncertainties



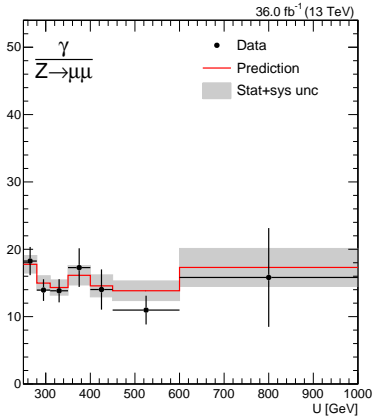
Large theoretical uncertainties

# Extrapolation uncertainties

$Z(\mu\mu)/Z(ee)$



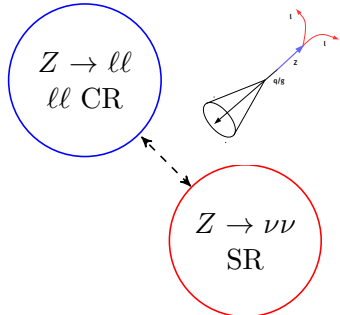
$Z(\mu\mu)/\gamma$



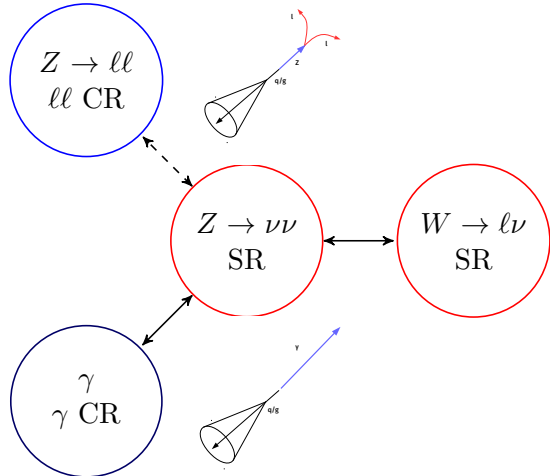
Small experimental uncertainties

Large theoretical uncertainties

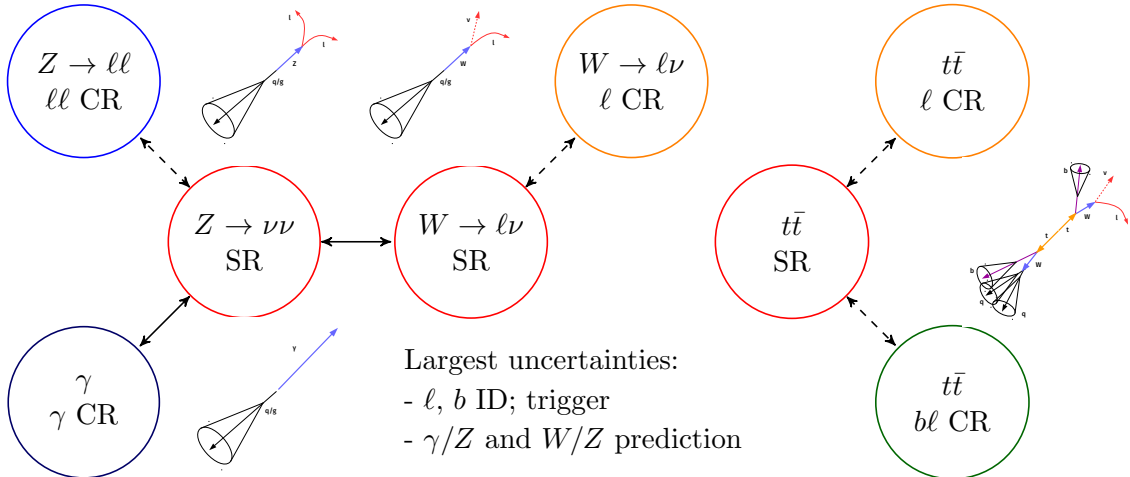
# Background estimation summary



# Background estimation summary



# Background estimation summary

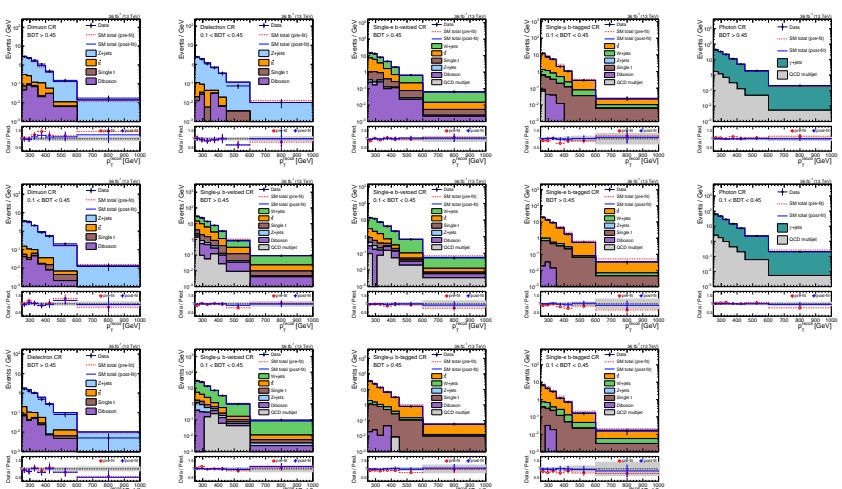
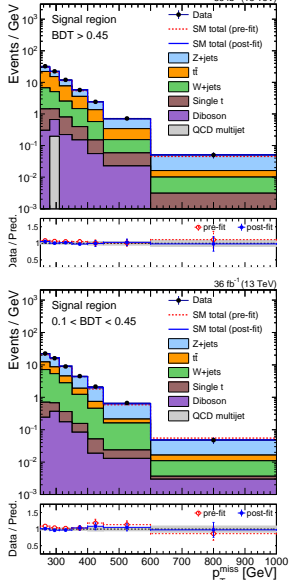


# Likelihood maximization

Likelihood assuming one major background ( $Z \rightarrow \nu\nu$ ) and one CR :

$$\begin{aligned}\mathcal{L}(\mathbf{d} \mid \mu, \boldsymbol{\mu}^Z, \boldsymbol{\theta}) = & \prod_i \text{Pois}\left(d_i^{\text{SR}} \mid \mu S_i(\boldsymbol{\theta}) + \mu_i^Z + B_i^{\text{SR}}(\boldsymbol{\theta})\right) \\ & \times \prod_i \text{Pois}\left(d_i^{\text{CR}} \mid \frac{\mu_i^Z}{T_i(\boldsymbol{\theta})} + B_i^{\text{CR}}(\boldsymbol{\theta})\right) \\ & \times \prod_j p(\theta_j)\end{aligned}$$

# MLE recoil distributions (SM hypothesis)

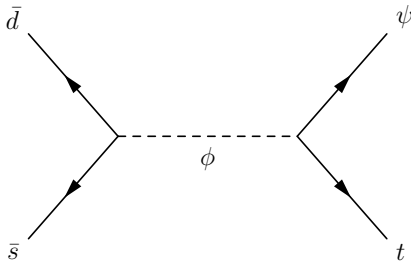


# Limits on mono-top benchmark models

Benchmark models probe range of mono-top kinematics.

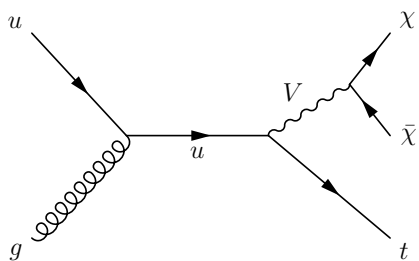
## Resonant scalar

- $p_T$  of top quark increases with  $m_\phi$
- Better selection efficiency at high  $m_\phi$



## FCNC

- Falling  $p_T^{\text{miss}}$  spectra  $\Rightarrow$  worse signal eff.
- Constraints on  $m_V$  and couplings  $g_\chi, g_q$

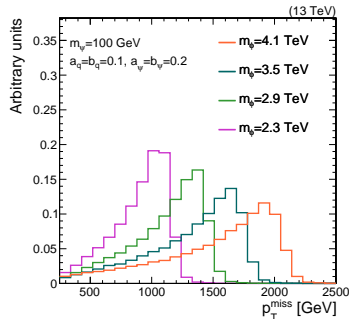


# Limits on mono-top benchmark models

Benchmark models probe range of mono-top kinematics.

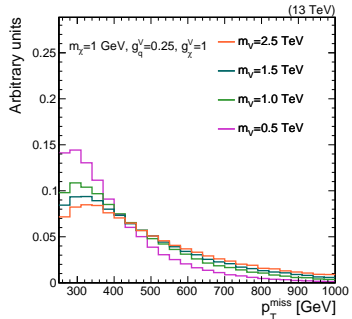
## Resonant scalar

- $p_T$  of top quark increases with  $m_\phi$
- Better selection efficiency at high  $m_\phi$



## FCNC

- Falling  $p_T^{\text{miss}}$  spectra  $\Rightarrow$  worse signal eff.
- Constraints on  $m_V$  and couplings  $g_\chi, g_q$



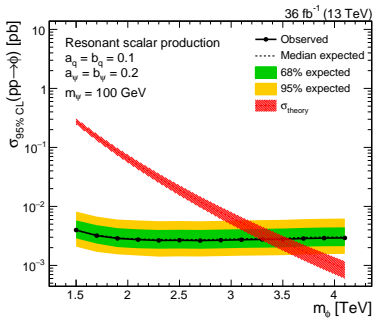
# Limits on mono-top benchmark models



Benchmark models probe range of mono-top kinematics.

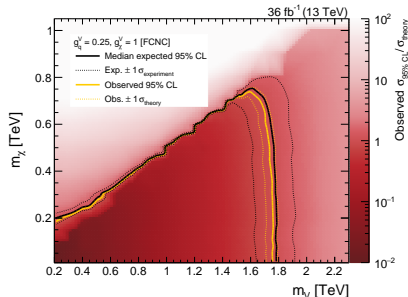
## Resonant scalar

- $p_T$  of top quark increases with  $m_\phi$
- Better selection efficiency at high  $m_\phi$



## FCNC

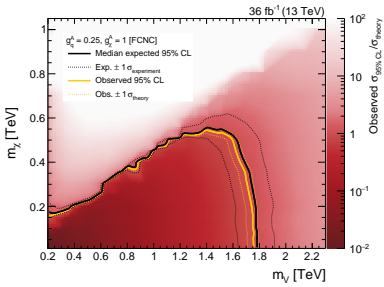
- Falling  $p_T^{\text{miss}}$  spectra  $\Rightarrow$  worse signal eff.
- Constraints on  $m_V$  and couplings  $g_\chi, g_q$



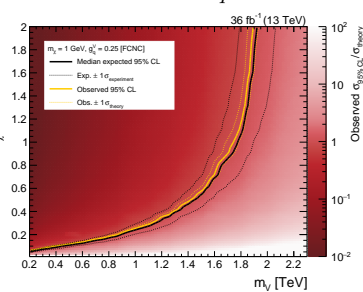
# FCNC parameter space

6 free parameters:  $m_\chi$ ,  $m_V$ ,  $g_q^V$ ,  $g_q^A$ ,  $g_\chi^V$ ,  $g_\chi^A$

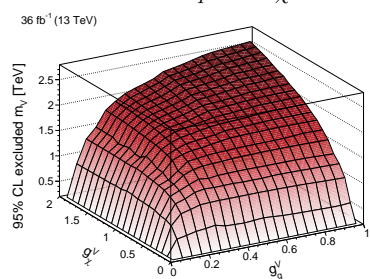
Axial-vector current



$m_V$  vs  $g_q^V$



$m_V$  vs  $g_q^V$  vs  $g_\chi^V$



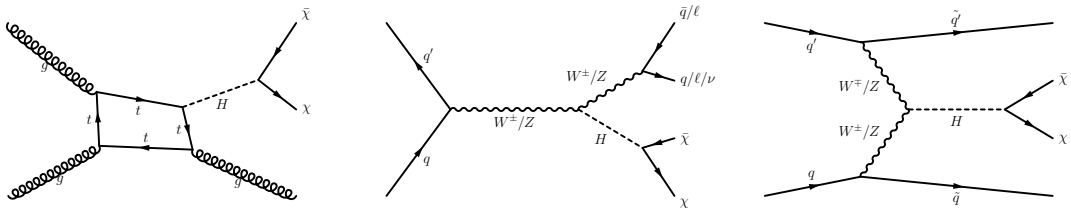
# Comparison to previous results

	CMS Run 1	This result
Dataset size	20/fb	36/fb
Collision energy	8 TeV	13 TeV
$\sigma(pp \rightarrow \phi \rightarrow t\psi)$ , $m_\phi = 1.5$ TeV	0.04 pb	0.19 pb
Reconstruction	3 resolved jets	1 merged jet
Excluded $m_\phi$	0.35 TeV	0.8-3.4 TeV
Excluded resonant $\sigma \times \mathcal{B}$	0.6 pb	0.002 pb
Excluded $m_V$	0.65 TeV	0.2-1.8 TeV
Excluded FCNC $\sigma \times \mathcal{B}$	0.2 pb	0.018 pb

# Vector boson fusion $H \rightarrow$ invisible

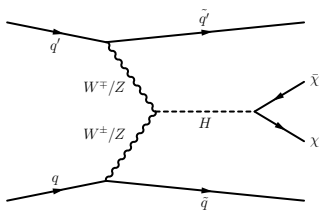
# Invisible Higgs

- ▶ Core assumptions:
  - ▶ DM mass generation is through Higgs mechanism
  - ▶  $2m_\chi < m_H$
- ▶ Production mode  $\Rightarrow$  mono-**X** channels
  - ▶  $gg \rightarrow H + \text{jet(s)} \Rightarrow \text{mono-jet}$
  - ▶  $VH \Rightarrow \text{mono-}V(qq') \text{ and mono-}Z(\ell\ell)$
  - ▶ Vector boson fusion  $\Rightarrow \text{VBF}+H \rightarrow \text{inv}$

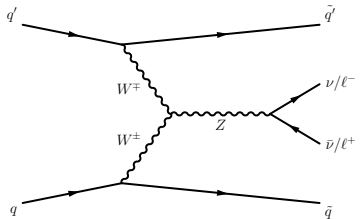


# Production of bosons with two jets

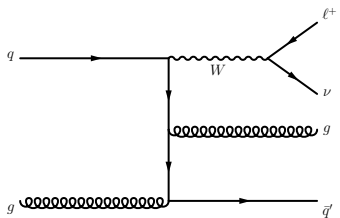
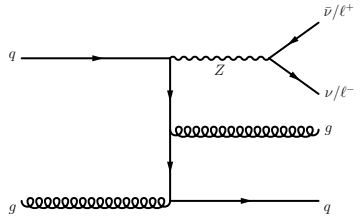
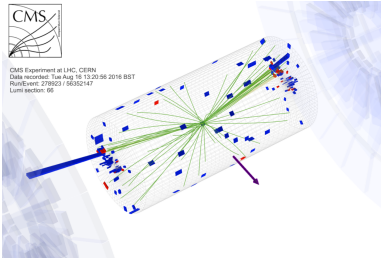
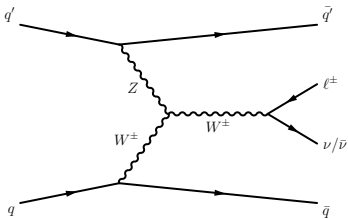
$$H \rightarrow \chi\bar{\chi}$$



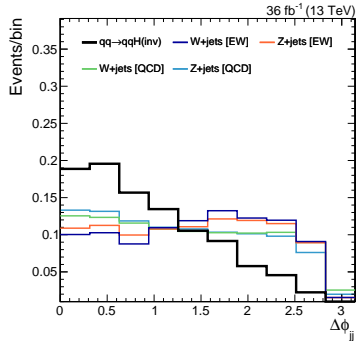
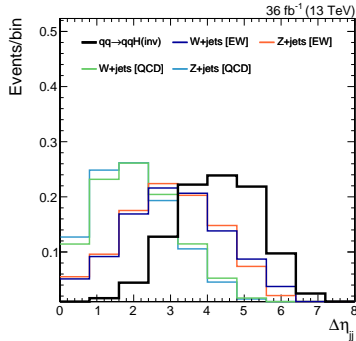
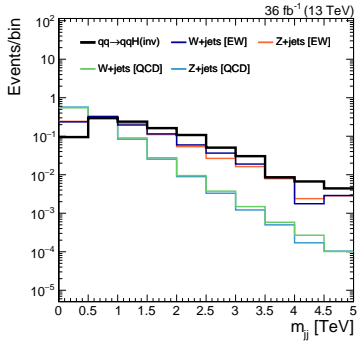
$$Z$$



$$W$$



# Dijet kinematics in QCD/EW/VBF processes



$\Delta\eta$  and  $m_{jj}$  strongly correlated

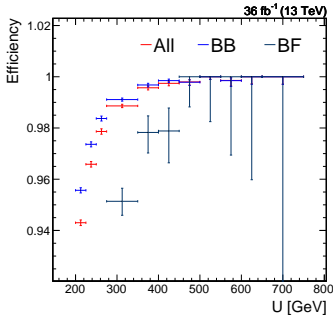
Use  $m_{jj}$  distribution to extract signal. Require  $\Delta\eta > 1$  and  $\Delta\phi < 1.5$ .

# Forward jets and L1 trigger

Resolution of  $p_T^{\text{miss}}$  strongly depends on location of jets

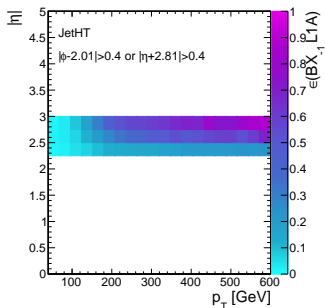
## L1 $p_T^{\text{miss}}$ calculation

- ▶ High rate from noise and multijet events
- ▶ Only  $|\eta| < 3$  particles



## L1 pre-firing

- ▶ Collisions are 25 ns apart
- ▶ Mis-timed signals block interesting events

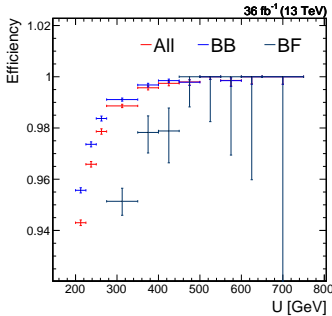


# Forward jets and L1 trigger

Resolution of  $p_T^{\text{miss}}$  strongly depends on location of jets

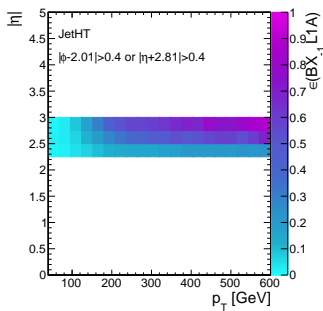
## L1 $p_T^{\text{miss}}$ calculation

- High rate from noise and multijet events
- Only  $|\eta| < 3$  particles



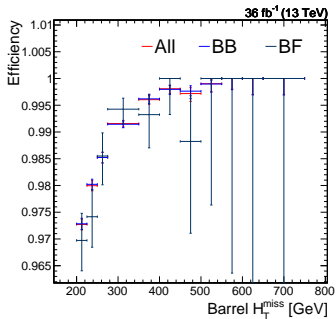
## L1 pre-firing

- Collisions are 25 ns apart
- Mis-timed signals block interesting events



## Net effect

- 20% of signal is lost when data is collected
- Fixed in 2018 data

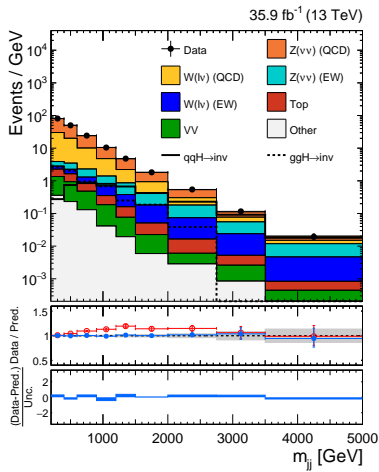
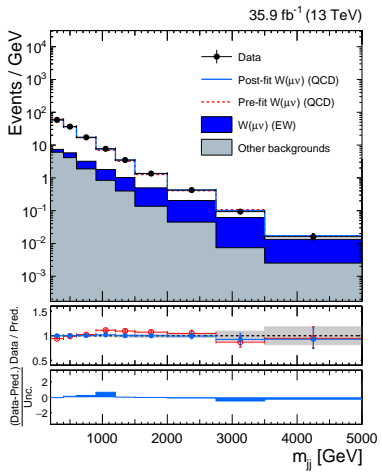


# $V$ +jet estimation



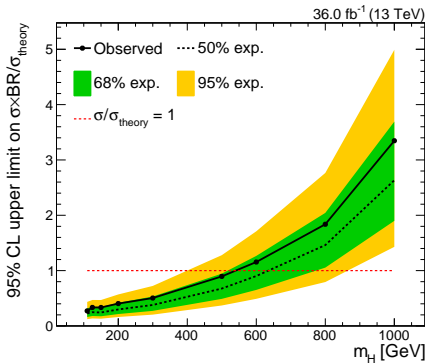
- Precision estimation of QCD and EW  $V$ +jets
- Similar strategy as mono-top, but no  $\gamma$  CR

Uncertainty	Size
$W/Z$ QCD	15%
$W/Z$ EW	15%
Trigger	2%
Lepton ID	2-3%

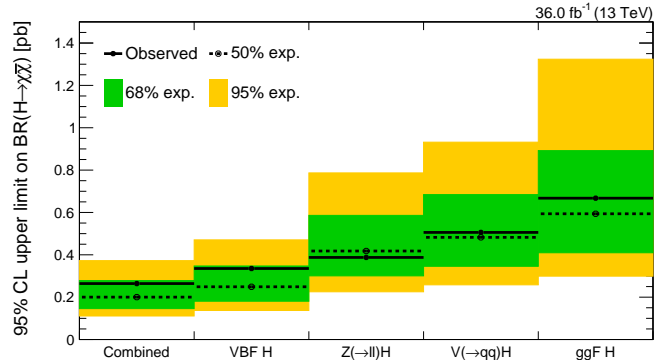


# Constraints on $\mathcal{B}(H \rightarrow \text{inv})$

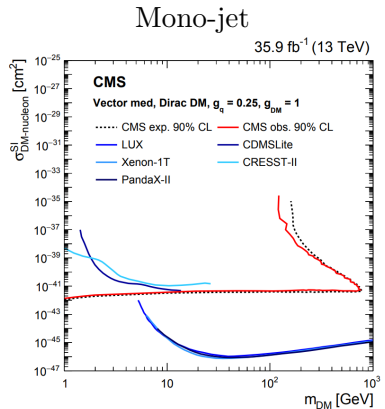
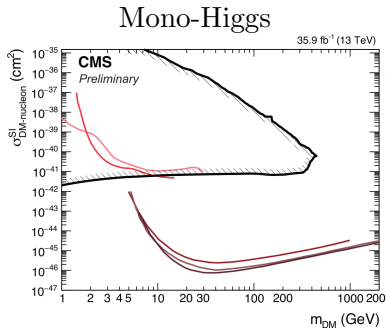
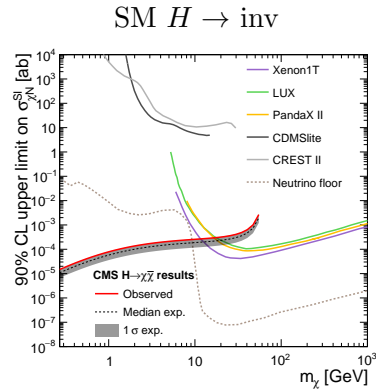
VBF-only



All production modes (SM Higgs)



# Comparison of LHC and direct detection constraints



- LHC constraints strongest at low DM mass
- Constraints depend strongly on choice of model

# Impact of analysis strategy and L1 losses



	Previous CMS result	This result
Collision energy	7,8,13 TeV	13 TeV
Dataset size	5,20,2/fb	36/fb
$\sigma(qq' \rightarrow qq'H)$	1.2,1.6,3.7 pb	3.7 pb
Exp. limit $\mathcal{B}(H \rightarrow \text{inv})$	0.30	0.25
Non-differential	-	0.30
No L1 effect	-	0.21

- ▶ Same sensitivity from old analysis technique on new dataset
  - ▶ Driven by losses in L1
- ▶ Improvements driven by precise measurement of EW+QCD  $V+\text{jet}$  spectra

# Improving DM searches at LHC: prediction of $V+jets$



VBF		
Uncertainty	Size	Effect
$W/Z$ EW	15%	50%
$W/Z$ QCD	15%	25%
Trigger	2%	20%
Lepton ID	2-3%	15%

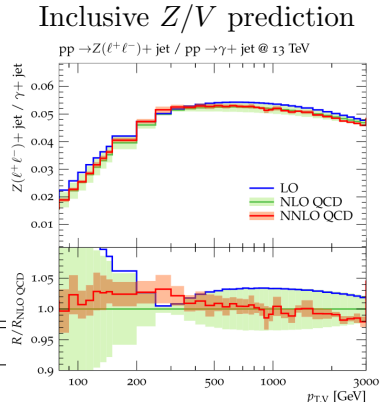
Mono-top		
Uncertainty	Size	Effect
$V/Z$ QCD	15%	30%
$b$ ID	2-10%	30%
Lepton ID	2-3%	15%

# Improving DM searches at LHC: prediction of $V$ +jets

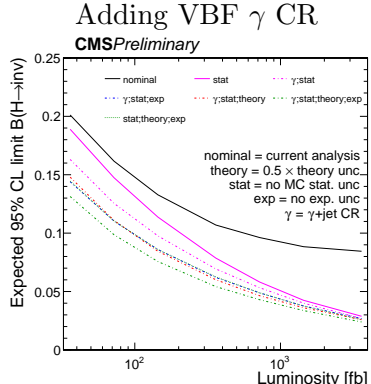


Uncertainty	VBF Size	Effect
$W/Z$ EW	15%	50%
$W/Z$ QCD	15%	25%
Trigger	2%	20%
Lepton ID	2-3%	15%

Uncertainty	Mono-top Size	Effect
$V/Z$ QCD	15%	30%
$b$ ID	2-10%	30%
Lepton ID	2-3%	15%



[10]



# Conclusions

## Mono-top

- ▶ Boosted top reconstruction extends reach
- ▶ Jet substructure is critical
- ▶ Strong constraints on flavor-changing DM models
- ▶ Substructure methods can be applied broadly

## VBF $H \rightarrow$ invisible

- ▶ Very different set of jet challenges: triggering, backgrounds, energy calibration
- ▶ Precise measurement of QCD and EW  $V$  spectra

# Conclusions

## Mono-top

- ▶ Boosted top reconstruction extends reach
- ▶ Jet substructure is critical
- ▶ Strong constraints on flavor-changing DM models
- ▶ Substructure methods can be applied broadly

## VBF $H \rightarrow$ invisible

- ▶ Very different set of jet challenges: triggering, backgrounds, energy calibration
- ▶ Precise measurement of QCD and EW  $V$  spectra

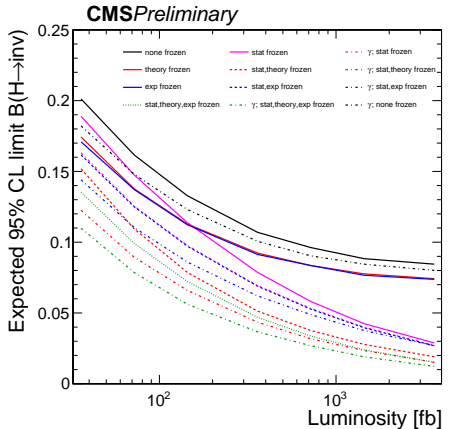
# Conclusions

## Mono-top

- ▶ Boosted top reconstruction extends reach
- ▶ Jet substructure is critical
- ▶ Strong constraints on flavor-changing DM models
- ▶ Substructure methods can be applied broadly

## VBF $H \rightarrow$ invisible

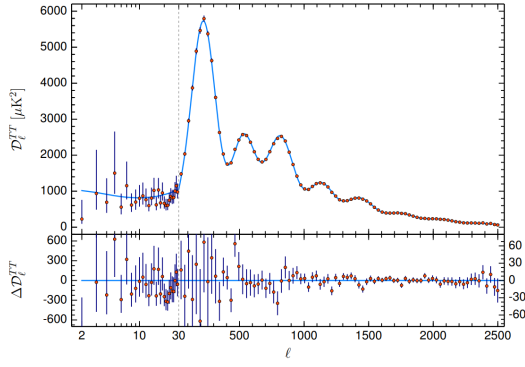
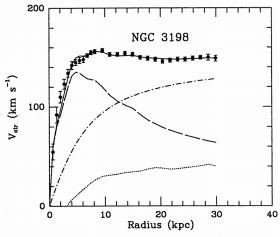
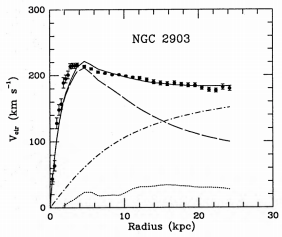
- ▶ Very different set of jet challenges: triggering, backgrounds, energy calibration
- ▶ Precise measurement of QCD and EW  $V$  spectra

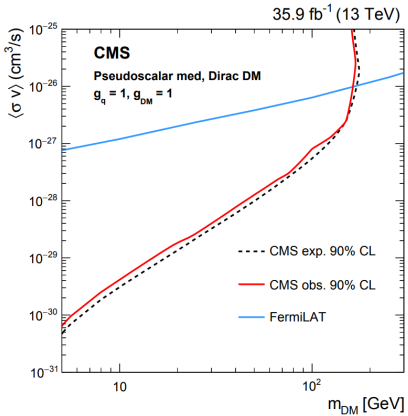
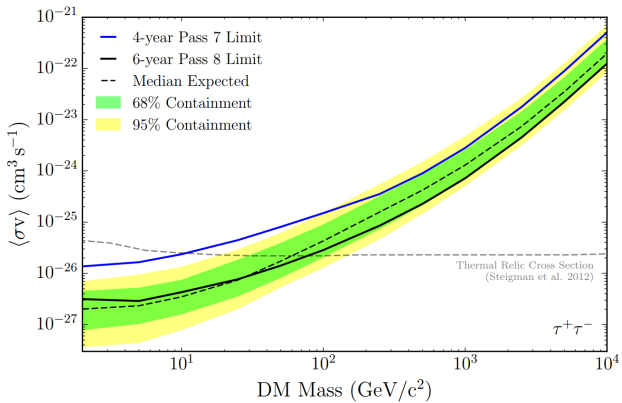


# BACKUP

# References

- [1] [https://en.wikipedia.org/wiki/Galaxy\\_rotation\\_curve](https://en.wikipedia.org/wiki/Galaxy_rotation_curve)
- [2] arXiv:astro-ph/9909252
- [3] hubblesite.org/image/1276/news\_release/2003-01
- [4] chandra.harvard.edu/photo/2006/1e0657/more.html
- [5] arXiv:astro-ph/1202.0090
- [6] [https://kipac.stanford.edu/highlights/  
let-there-be-light-upon-dark-digging-deeper-dark-matter-lux](https://kipac.stanford.edu/highlights/let-there-be-light-upon-dark-digging-deeper-dark-matter-lux)
- [7] <https://fermi.gsfc.nasa.gov/science/eteu/dm/>
- [8] <https://cms-docdb.cern.ch/cgi-bin/PublicDocDB>ShowDocument?docid=4172>
- [9] arXiv:1609.07473
- [10] arXiv:1705.04664





## LHC luminosity

$$L = \frac{N_b^2 n_b f_{\text{rev}} \gamma F}{4\pi \epsilon \beta^*}$$

- ▶  $N_b$  = particles per bunch
- ▶  $n_b$  = bunches per beam
- ▶  $f_{\text{rev}}$  = frequency of revolution
- ▶  $\gamma = E/m$  of beam
- ▶  $\epsilon$  = emittance of beam
- ▶  $\beta^*$  = beta function at collision point
- ▶  $F$  = factor accounting for beam intersection geometry

